

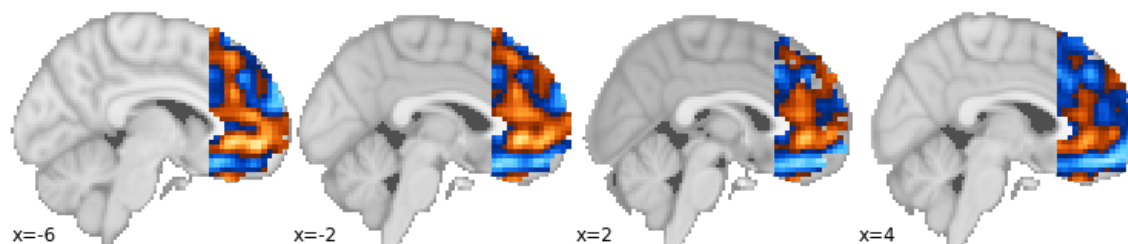
Supplementary Materials

To contextualize the back-projected model weights from our Ridge-PCR, we compare their magnitude and direction with a mass univariate contrast of Self > Other. For each participant we performed a linear contrast between self and other conditions using the general linear model as implemented in SPM8. Individual contrast images were entered into a second-level model to estimate the average effect across participants. Visual inspection (Figure S1) indicates a similar pattern of weights between the Ridge-PCR model and the Self > Other contrast, and a correlation of these voxel weights results in a Pearson R of 0.51 ($p < 0.001$), indicating moderate similarity (Figure S3).

In addition to this analysis, we created a mask for those voxels that were reliably predictive from our Ridge-PCR model, which included a cluster in the OFC, VMPFC, and a small group of voxels in the DMPFC. We then used this map to isolate the contrast values in the Self > Other group contrast map, and compared the sign of this array with the sign of these same voxels from the Ridge-PCR model. This comparison gives a 98% match (Figure S2).

Together these comparisons indicate that the map of weights from our main analysis are meaningful and consistent with activation based analysis, and that the maps we present provide useful information for understanding how the brain represents and encodes self and other related thought.

A.



B.

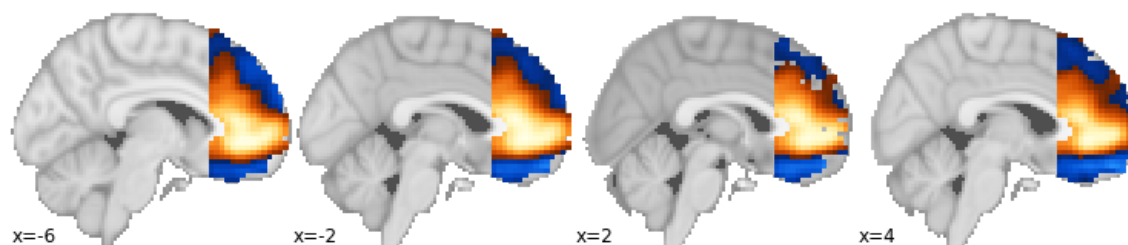


Figure S1: Comparison of voxel weights between Ridge-PCR analysis and mass univariate Self > Other contrast. (A) Map of relative voxel weights for Ridge-PCR predictive model. (B) Map of mass univariate contrast for Self > Other conditions.

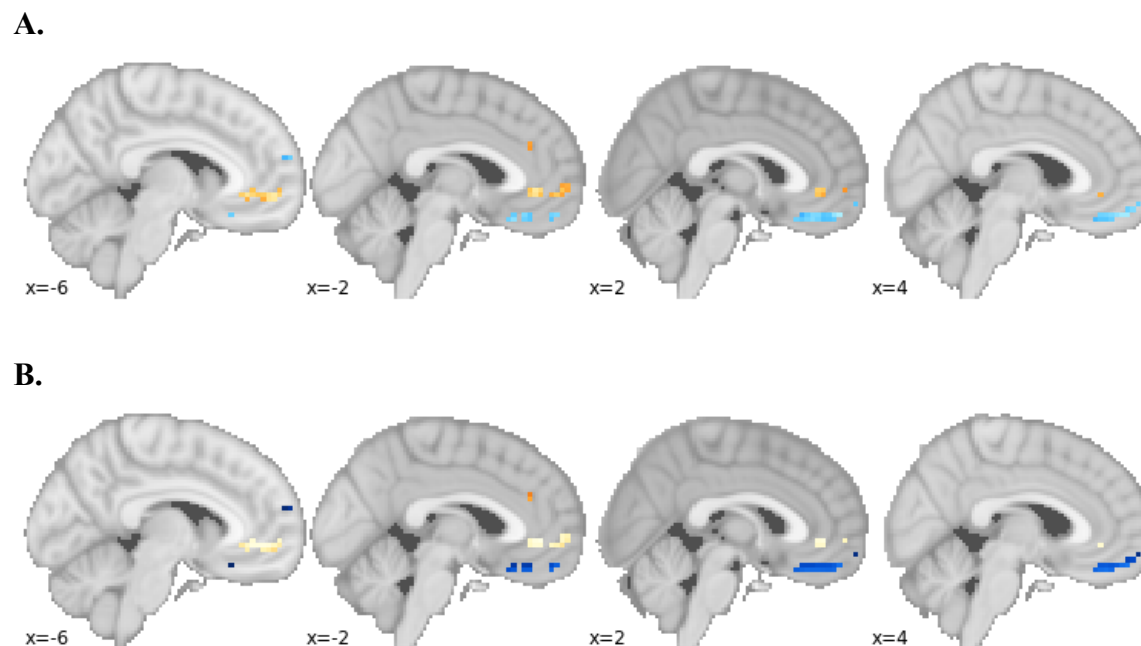


Figure S3: Comparison of voxel weights between Ridge-PCR analysis and mass univariate Self > Other contrast within those voxels passing FDR correction from Ridge-PCR model (A) Map of above threshold voxel weights for Ridge-PCR predictive model. (B) Map of mass univariate contrast for Self > Other conditions within voxels that passed threshold test for Ridge-PCR analysis. Comparing the sign of these voxels returns a 98% overlap in directional encoding for self and other related processing.

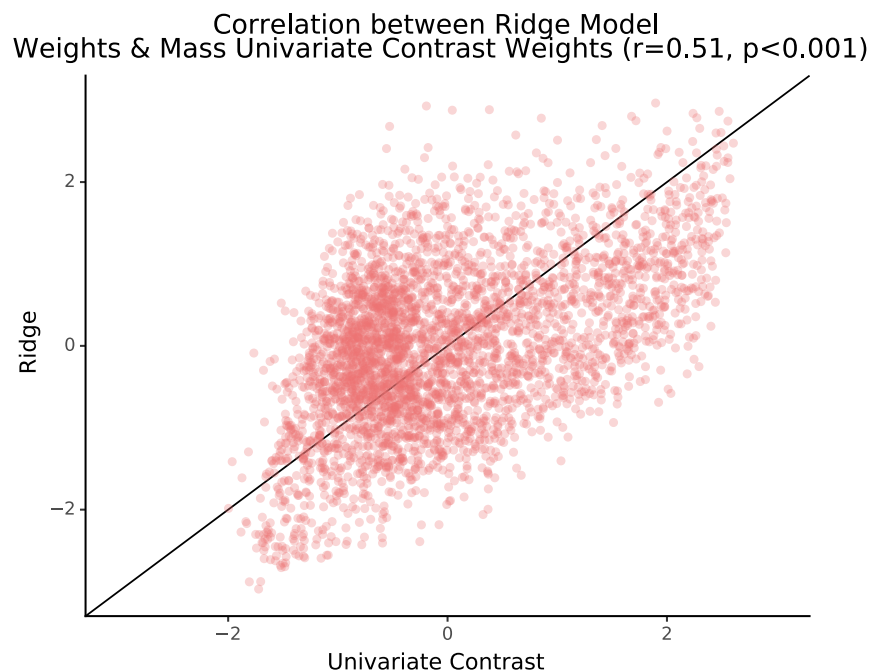


Figure S3: Ridge-PCR regression coefficients from the main analysis were back projected into the 3-D MPFC mask. Additionally, the z-map from a mass univariate contrast of self > other for all three studies was projected into the same space. These two patterns were compared via a Pearson correlation, which resulted in a robust, moderate to strong association ($r = 0.51$, $p < 0.001$), indicating that the relative voxel weights of the predictive model and the voxel weights from the mass univariate analysis resulted in similar spatial organizations.

In addition to Ridge-PCR, we employed two alternative machine learning models for comparison and to ensure that our results were robust to methodological choices. Specifically, we repeated our Ridge-PCR analysis but substituted an SVC model (SVC-PCA), and performed a partial least squared discriminant analysis (PLS-DA). Model hyperparameters (C parameter for SVC, number of components for PLS-DA) were tuned using the same stratified 5-fold cross-validation as our original model, and the best performing model was retrained on the entire training set before being carried forward for out-of-sample prediction. Out-of-sample prediction was carried out through a bootstrap procedure in which 1,000 samples were drawn with replacement to obtain confidence intervals for the test-accuracy. Additionally, permutation tests were performed for these two models to identify voxels within the MPFC that most robustly contributed to the model performance. Both models had very similar performance out-of-sample (Table S2). For PLS-DA, a model with 4 components was best able to explain the most variance in our dependent variable (self or other related trial), indicating that four latent components are sufficient to describe the dimensionality of the processes contributing to discriminating between self- and other-related thought. Finally, the organization of model weights are also consistent with our main results (figure S4), further bolstering the findings from our main analysis.

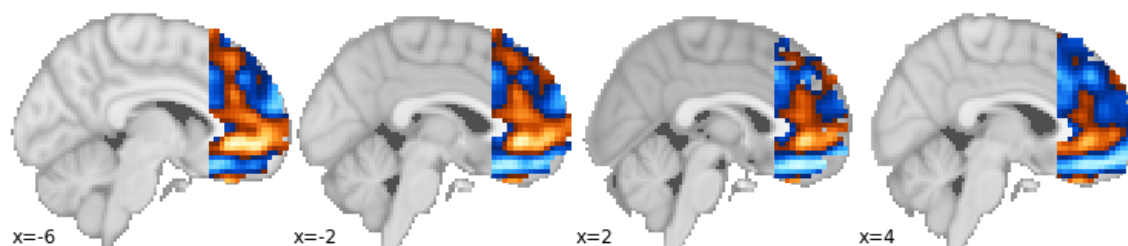
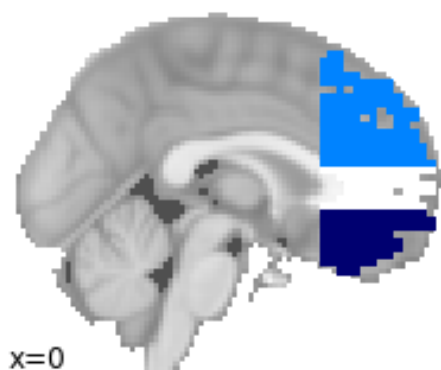


Figure S4: Map of voxel-weights in MPFC from PLS-DA with 4 components.



Figures S5: Segmentation of the MPFC into VMPFC, mid-MPFC, and DMPFC for local average predictive logistic regression. The average activation for each of these ROI was extracted for all observations used in the main analysis of the paper. The same procedures were used to train and test this model as those in the main paper. The ROI predictive model returned an out-of-sample accuracy of 0.52% (SD = 2.9), indicating that the average signal from these regions is insufficient for robust prediction of self and other related thought. The sign of these three ROI, however, were somewhat consistent with the organization found in the main Ridge-PCR analysis, wherein the VMPFC and DMPFC had negative sign and the mid-MPFC had positive sign.

Model	Accuracy
Ridge-PCR	63.7% (min=57%, max=66%)
SVC-PCA	61.2% (min=58%, max=65%)
PLS-DA	64.3% (min=57%, max=69%)

Table S1: 5-fold cross-validation training accuracy scores for Ridge-PCR main analysis using data from the MPFC. Ridge-PCR is compared to SVC-PCA and PLS-DA models to establish the reliability and robustness of the results obtained in the main analysis.

Model	Accuracy
Ridge-PCR	58.9% CI = [54%, 64%]
SVM-PCA	59.8% CI = [54%, 66%]
PLS-DA	60.1% CI = [55%, 66%]

Table S2: Out of sample test accuracy for Ridge-PCR main analysis using data from the MPFC. Ridge-PCR is compared to SVC-PCA and PLS-DA models to establish the reliability and robustness of the results obtained in the main analysis. Mean and CI for test accuracy were derived through bootstrapping with replacement on the held-out test set.

Model	Accuracy
Ridge-PCR	71.8% (min=67%, max=75%)
SVM-PCA	70.0% (min=68%, max=73%)
PLS-DA	71.0% (min=69%, max=74%)

Table S3: 5-fold cross-validation training accuracy scores for Ridge-PCR main analysis using data from the whole brain. Ridge-PCR is compared to SVC-PCA and PLS-DA models to establish the reliability and robustness of the results obtained in the main analysis.

Model	Accuracy
Ridge-PCR	67.7% CI = [62%, 73%]
SVM-PCA	63.6% CI = [58%, 69%]
PLS-DA	69.5% CI = [64%, 74%]

Table S4: Out of sample test accuracy for Ridge-PCR main analysis using data from the whole brain. Ridge-PCR is compared to SVC-PCA and PLS-DA models to establish the reliability and robustness of the results obtained in the main analysis. Mean and CI for test accuracy were derived through bootstrapping with replacement on the held-out test set.

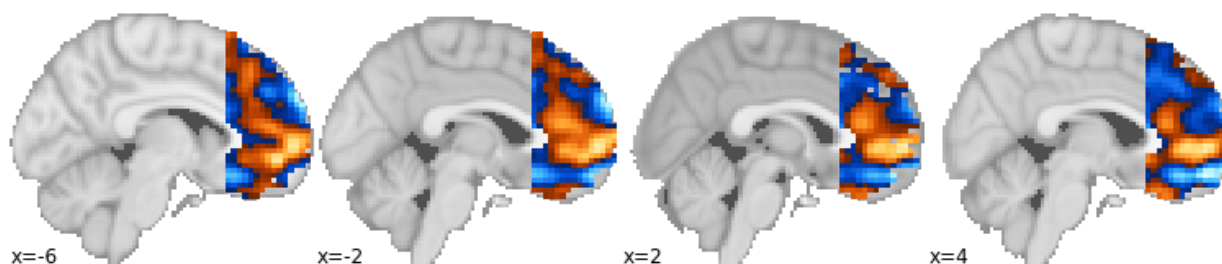
Table S5: Study Participant Demographics

	Training Sample	Testing Sample
	$N = 111$	$N = 31$
Age	$M = 29.25, SD = 12.52$	$M = 31.00, SD = 13.25$
Sex (% female)	55%	55%
Ethnicity		
	White	57%
	Black	15%
	Asian	10%
	Latino	5%
	Multiracial	5%
	Other/Not Specified	8%

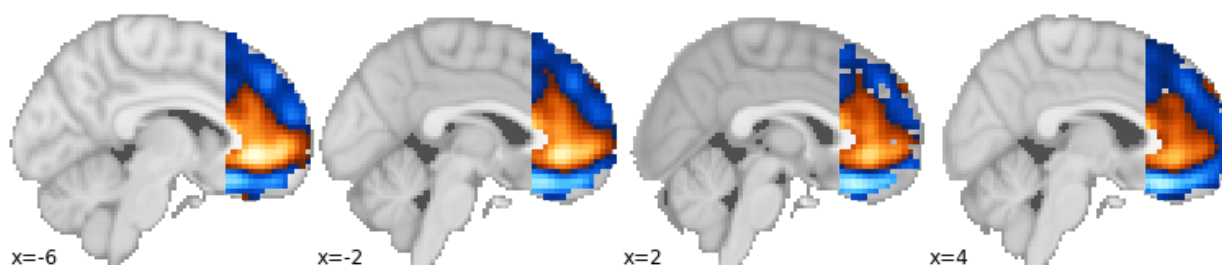
**units are individual participants*

To better understand how each of the three studies in our dataset contributed to the performance of our main classification model, we retrained a Ridge-PCR model on each dataset independently. We see from the unthresholded maps that study 1 and 2 were most influential, but that study 3 did not have a consistent pattern of results. In addition to this, the model trained on data from study 3 did not perform as well as study 1 or 2. There are multiple potential reasons for this result, namely that the task implemented in study 3 differed from study 1 and 2, and that there were substantially fewer trials from study 3 ($n = 270$) compared to study 1 ($n = 707$) and study 2 ($n = 468$). Figure S6 shows the MPFC model weights for each study.

A.



B.



C.

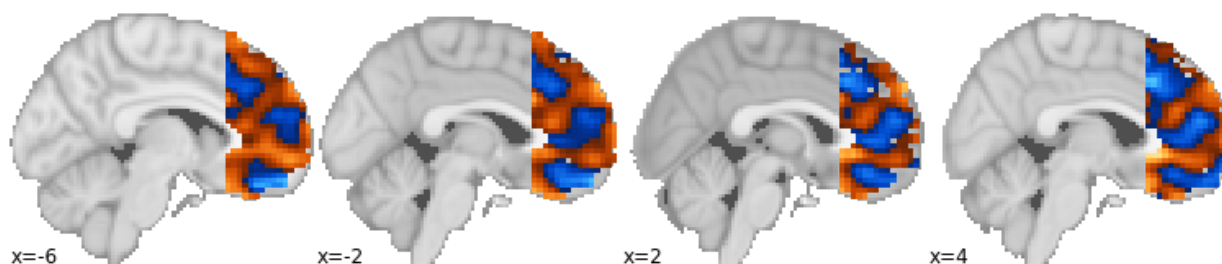


Figure S6: unthresholded MPFC voxel weight maps for Ridge-PCR trained on each of the three studies independently. A) weight map for study 1, B) weight map for study 2, C) weight map for study 3.